JOURNAL OF AIRCRAFT
Vol. 30, No. 5, Sept.–Oct. 1993

Identification of Actuation System and Aerodynamic Effects of Direct-Lift-Control Flaps

R. V. Jategaonkar*
Institute of Flight Mechanics, DLR, Braunschweig, Germany

A maximum likelihood parameter estimation method for nonlinear systems has been applied to flight data of the research aircraft ATTAS (advanced technologies testing aircraft system). The emphasis is on modeling and identification of 1) dynamics and nonlinearities of actuation systems for the direct-lift-control (DLC) flaps, and 2) their aerodynamic effectiveness and other influences. These specially designed flaps provide an additional longitudinal control suitable for in-flight simulation or load alleviation investigations. The identification results indicate that under aerodynamic loads the possible maximum flap deflections are severely limited. The flight-estimated aerodynamic characteristics are compared with those predicted by wind tunnel and analytical methods. It is found that the DLC flaps are somewhat less effective aerodynamically than they were designed for. More importantly, the transit time lag in the downwash generated due to flap deflections significantly affects the dynamic pitching motion. Furthermore, it leads to certain additional unsymmetrical and interference effects.

Introduction

AT the German Aerospace Research Establishment (DLR) during the last couple of years, an advanced technologies testing aircraft system (ATTAS) was developed by modifying a medium-size, twin-engine, short-haul 44-passenger aircraft of the type VFW-614, Fig. 1.[1] This research aircraft serves as the primary flight vehicle for flight control research, handling qualities investigations, pilot-in-the-loop evaluations, and system assessment.[2–4] It is equipped with a wide range of sophisticated sensors, instrumentation, and electronics. One of the major features of the aircraft modifications is that, in addition to the conventional controls, the ATTAS aircraft is equipped with direct-lift-control (DLC) flaps for high-frequency direct-lift modulation, (Figs. 1 and 2). A detailed description of the research aircraft ATTAS and of its various modifications is neither within the scope of this article nor is it required for the problem addressed here.

It is, in general, well known that the DLC flaps provide an additional independent longitudinal control, which is particularly suitable and necessary for realistic in-flight simulations (i.e., simulation of other aircraft in flight). The fidelity of the in-flight simulator, particularly incorporating modern control concepts, depends to a very large extent on the accuracy of the mathematical model representing the host aircraft, and as such the demands on the modeling accuracy are very high.[5,6] This is true not only of the aerodynamic model but also of the actuation systems. Therefore, in the case of ATTAS aircraft, a flight-validated accurate knowledge of its aerodynamic characteristics and actuator dynamics is considered a prerequisite for successful flight investigations, as well as for ground-based simulator.

Although the analytical methods and wind-tunnel tests usually provide reasonable predictions of the aerodynamic characteristics, the importance and advantages of validating and, if necessary, updating these predictions with those estimated from flight test data are, in the field of aircraft stability and control, well-recognized.[6–8] Furthermore, in the present case, the aircraft motion in response to identical control inputs in flight and in a simulation incorporating the predicted aerodynamic data showed some noticeable discrepancies,[9] thereby necessitating the aerodynamic model identification from flight data using system identification methods. The advanced system identification methods provide a convenient tool to model from a set of input-output observations, the cause-effect relationship purported to underlie the physical phenomenon under investigation.[8,10,11]

In order to achieve the above general objective, a comprehensive flight test program for gathering data was carried

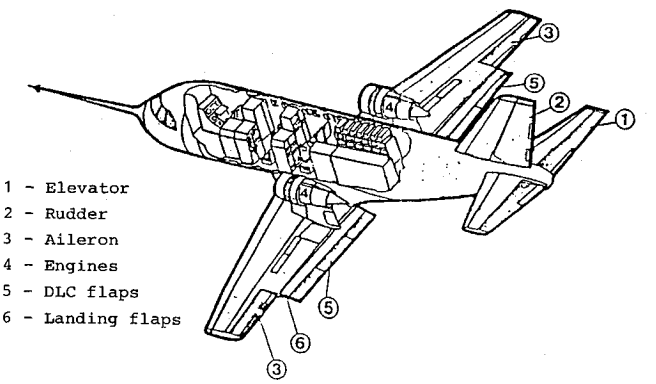

Fig. 1 Research aircraft ATTAS.

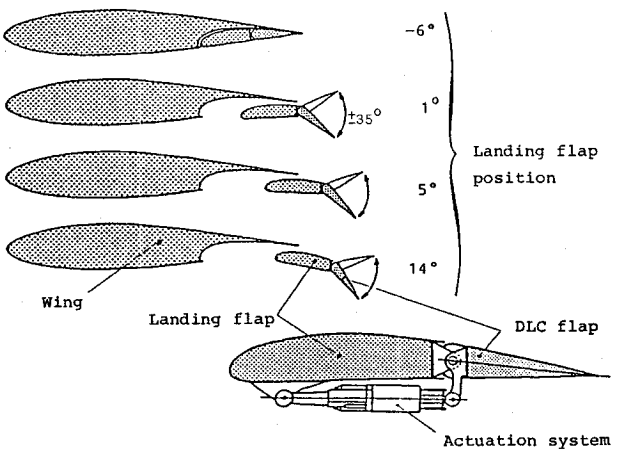

Fig. 2 DLC flaps.

Received Dec. 23, 1991; presented as Paper 92-0171 at the AIAA 30th Aerospace Sciences Meeting and Exhibit, Reno, NV, Jan. 6–9, 1992; revision received March 25, 1992; accepted for publication May 21, 1992.

*Research Scientist, Mathematical Methods and Data Handling Branch.

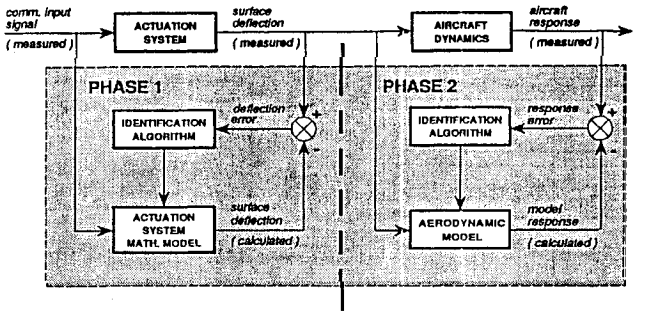

Fig. 3 Block schematic of ATTAS system identification.

out with the research aircraft ATTAS.[12] In this article, the attention is mainly focused on the following two aspects: 1) identification of dynamics and nonlinearities in the DLC-flap actuation system, and 2) modeling and estimation of aerodynamic effectiveness and of other influences, such as unsteady, unsymmetrical, and interference effects of the DLC-flaps. For both of these purposes, a parameter estimation method for nonlinear systems based on the maximum likelihood principle is applied.[10,13] The flight-estimated aerodynamic characteristics are compared with those predicted by wind-tunnel measurements.

DLC-Flap Configuration

The DLC flaps are derived by modifying a trailing-edge portion (45%) of the landing flaps, see Figs. 1 and 2. They are divided into six fast-moving flaps, three on each wing. Each of the six flaps is driven by an individual electrohydraulic actuation system which is both rate- and force-limited for structural safety reasons. The six flaps are designed for a maximum deflection of ±35 deg and for an actuation rate of 75 deg/s under aerodynamic loads. The DLC flaps can be operated for landing-flap deflections between 1–14 deg. Simultaneous variations of the DLC and landing flaps are possible.

The flight test program for system identification is carried out in two phases (Fig. 3).[4,12] In the first phase, flight tests, input signals, and the onboard data recording were optimized for identification of the actuation system. In the second phase, the attention is mainly focused on the identification of rigid-body aerodynamics. Identification algorithm is based on the maximum likelihood output error method (see the Appendix).

DLC-Flap Actuation System

The flight investigations carried out showed that for small amplitudes, i.e., in the linear range, the DLC-flap actuation system can be adequately modeled as a second-order system. To extend the linear model to cover a wider range of operation, rate and displacement limitations need to be included (Fig. 4).[14,15] Furthermore, it is also found that the system gain is a function of the aerodynamic loading. In a general case, the mathematical model can be represented as

$$\ddot{\eta}_{DLC}(t) + 2\zeta\omega_n\dot{\eta}_{DLC}(t) + \omega_n^2\eta_{DLC}(t) = K(\bar{q})\omega_n^2 u(t) \quad (1)$$

with

$$|\dot{\eta}_{DLC}(t)| \leq \dot{\eta}_{max} \quad (2a)$$

$$\eta_{DLC}^{min} \leq \eta_{DLC} \leq \eta_{DLC}^{max} \quad (2b)$$

where η_{DLC} denotes the DLC-flap deflection, u the commanded deflection (input), $\dot{\eta}_{max}$ the rate limitation, η_{DLC}^{min} and η_{DLC}^{max} the maximum negative (up) and positive (down) deflections, ω_n the natural frequency, ζ the damping ratio and $K(\bar{q})$ the gain as a function of dynamic pressure $\bar{q}$.

To identify the unknown parameters of the dynamic system, and also the unknown rate limitation $\dot{\eta}_{max}$ and saturation

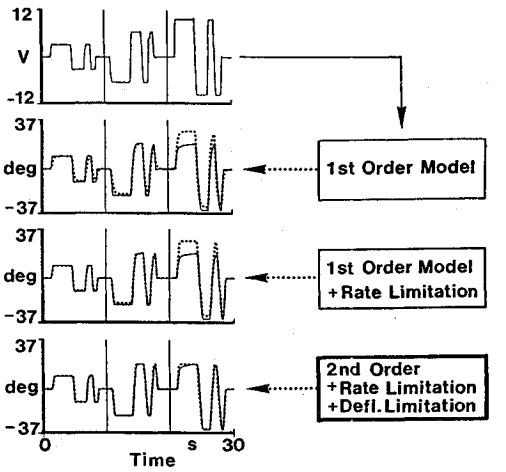

Fig. 4 Modeling of DLC-flap actuator dynamics.

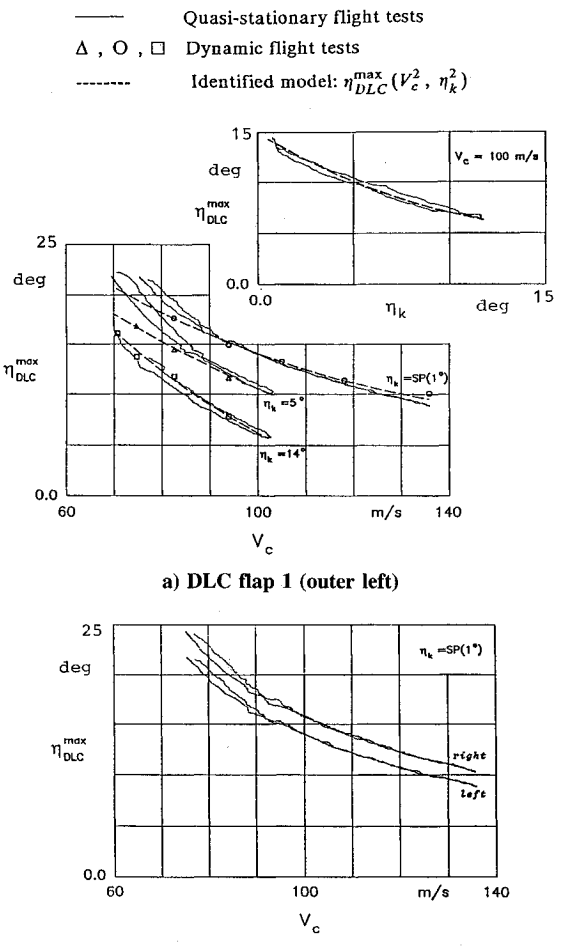

a) DLC flap 1 (outer left)

b) DLC flaps 1 and 6 (outer left and right)

Fig. 5 Maximum deflection of the DLC flaps.

limits η_{DLC}^{min} and η_{DLC}^{max}, a special flight-test program consisting of quasistationary and dynamic flight tests was carried out. The parameters of the dynamic model, Eq. (1), were estimated from dynamic maneuvers with a relative standard deviation (Cramer-Rao bounds[16]) of less than 0.5%. Estimation of the gain parameter $K(\bar{q})$ required combining multiple time records at several flight conditions.

The flight investigations show that the possible maximum deflection of DLC flaps is limited and depends upon the landing-flap position and aerodynamic loads acting on the aircraft. The aerodynamic loads in excess of the force limitation of the actuators result in deflection limitation. For example, Fig. 5a

shows the flight measured maximum DLC-flap deflection, η_{DLC}^{max}, as a function of calibrated airspeed V_c, and landing flap position η_k. Quasistationary flight maneuvers (i.e., tests with steady and slow variations in the two influencing variables, namely the dynamic pressure and landing flap position), as well as dynamic flight maneuvers (i.e., tests with rapidly changing multistep DLC inputs), are shown.

For the flight configurations tested here, it can be observed from Fig. 5 that (depending upon the flight condition) the maximum DLC-flap deflection can be limited from 10 to 22 deg for a landing-flap position of $\eta_k = 1$ deg. For other landing-flap positions, the possible maximum deflection is even smaller than that for $\eta_k = 1$ deg. DLC-flap deflections in the range of 10–15 deg are not uncommon for the various flight applications.

Since the basic purpose of the DLC flaps is high-frequency direct-lift modulation, the measurements from dynamic tests are further used to model nonlinearities in the possible maximum DLC-flap deflections and to estimate the unknown parameters in the postulated model. Since the dynamic maneuvers are carried out at a preselected flight condition, they usually provide a discrete test point (Fig. 5a). Therefore, it sometimes becomes difficult to postulate an appropriate model structure for the nonlinearities. In the present case, the quasistationary tests are used to obtain the nature of nonlinearities, which in this case is observed to be quadratic both in airspeed and landing flap deflection. Mathematically it can be represented as

$$\eta_{DLC}^{max} = \eta_{DLC\text{-}max} + K_{V1}^{+}V_c + K_{V2}^{+}V_c^2 + K_{\eta 1}^{+}\eta_k + K_{\eta 2}^{+}\eta_k^2 + K_{V\eta}^{+}V_c\eta_k \quad (3a)$$

$$\eta_{DLC}^{min} = \eta_{DLC\text{-}min} + K_{V1}^{-}V_c + K_{V2}^{-}V_c^2 + K_{\eta 1}^{-}\eta_k + K_{\eta 2}^{-}\eta_k^2 + K_{V\eta}^{-}V_c\eta_k \quad (3b)$$

Without going into any further details, it would suffice to mention here that the various parameters appearing in Eqs. (3) are estimated separately for each of the six DLC-flaps from flight data applying a nonlinear maximum likelihood parameter method. The identified model for the outermost flap (shown by dashed lines in Fig. 5a) agrees fairly well with the dynamic test measurements. Some discrepancies are observed for quasistationary flight at larger deflections, which may be attributed to the internal friction in the actuators. To obtain uncorrelated estimates of the parameters appearing in Eq. (3), it was necessary to analyze several flight conditions simultaneously. These parameters were estimated with a standard deviation of 2–5%.

Estimation of rate limitation, $\dot{\eta}_{max}$, from dynamic maneuvers with rapidly changing inputs commanding significantly higher rates than $\dot{\eta}_{max}$, was fairly straightforward. When reached, the rate limits are known to introduce response time lags. It can be concluded that the identified model adequately characterizes the nonlinearities in maximum DLC-flap deflection.

Aerodynamics of DLC Flaps

As an integral part of the complete aerodynamic modeling from flight data, the aerodynamic effectiveness and other effects due to the DLC flaps are identified along with the other aerodynamic derivatives pertaining to the longitudinal and lateral-directional motion. For this purpose, several flight maneuvers with appropriate elevator, horizontal stabilizer, engine throttle, aileron, rudder, and DLC-flap inputs at different reference flight conditions are combined together.[12] A multiple-maneuver analysis, applying maximum likelihood method, enables the estimation of a single set of aerodynamic derivatives common to all of the flight maneuvers analyzed. Parameter estimation is carried out based on the coupled six degree-of-freedom equations of aircraft motion formulated in a body-fixed axes system.[16] As already pointed out, the details of aerodynamic modeling for the DLC flaps are presented here.

For the purpose of aerodynamic modeling, the six DLC flaps are considered in two units, each consisting of three flaps on each wing, hereafter called left and right DLC flaps. Equivalent left and right DLC-flap deflections, denoted respectively by η_{DLC}^{L} and η_{DLC}^{R}, are computed from the individually measured flap deflections proportional to the surface areas.[12]

The total variations in the lift, drag, and pitching moment coefficients, C_{LDLC}, C_{DDLC}, and C_{mDLC} due to the DLC flaps are given by

$$C_{LDLC} = \Delta C_{LDLC}^{L} + \Delta C_{LDLC}^{R} \quad (4a)$$

$$C_{DDLC} = \Delta C_{DDLC}^{L} + \Delta C_{DDLC}^{R} \quad (4b)$$

$$C_{mDLC} = \Delta C_{mDLC}^{L} + \Delta C_{mDLC}^{R} + \Delta C_{mDLC}^{\varepsilon} \quad (4c)$$

where the contributions due to the left and right DLC flaps are denoted by superscripts L and R, respectively. The following general model for these contributions is postulated[12,14]:

$$\Delta C_{LDLC}(\eta_{DLC}) = A_1\eta_{DLC} + A_2\eta_{DLC}^2 + A_3\eta_{DLC}^3 \quad (5a)$$

$$\Delta C_{DDLC}(\eta_{DLC}) = (W_1 + W_{1\alpha}\alpha)\eta_{DLC} + W_2\eta_{DLC}^2 \quad (5b)$$

$$\Delta C_{mDLC}(\eta_{DLC}) = M_1\eta_{DLC} + M_2\eta_{DLC}^2 + M_3\eta_{DLC}^3 \quad (5c)$$

where A_i, W_i, and M_i are the unknown aerodynamic derivatives which are to be estimated from flight data. Furthermore, in Eq. (4c), $\Delta C_{mDLC}^{\varepsilon}$ denotes the downwash lag effect due to deflection of the DLC flaps. As will be demonstrated in this article, the system identification results have clearly brought out the need to account for this unsteady aerodynamic effect. The downwash lag effect $\Delta C_{mDLC}^{\varepsilon}$ is modeled as

$$\Delta C_{mDLC}^{\varepsilon} = C_{L\varepsilon}(r_H^*/l_\mu)M_\tau\eta_{DLC}(t - \tau) \quad (6)$$

where $C_{L\varepsilon}$ denotes the stabilizer lift coefficient, ε the stabilizer trim angle, r_H^* the horizontal distance between the neutral points of the wing and of the tail, and l_μ the aerodynamic mean chord. Furthermore, $\eta_{DLC}(t - \tau)$ denotes the time-delayed signal $\eta_{DLC}(t)$, with $\tau = r_H^*/V$ representing the transit time required for any flow modification generated at the wing to reach the tail, and M_τ the unknown downwash parameter.

As elaborated in the foregoing section, the nonlinearities in the possible maximum DLC-flap deflection are evident from Fig. 5a. These nonlinearities, although important for modeling of DLC-flap actuation system, are not directly relevant to aerodynamic modeling, since the actual flight measured surface deflections are used in the aerodynamic modeling and identification (phase 2 of Fig. 3). The actual forces and moments generated depend only on the actual flap deflection, and not on the commanded input. However, Fig. 5b shows that even though the DLC flaps are configured for symmetrical operation, the possible maximum deflections of the left and right DLC flaps resulting from the same commanded input are unequal. Such unequal deflections are allowed within a small permissible tolerance limit. Such a tolerance band helps to account for the differences in mechanical assembly as well as in static and dynamic response characteristics of the six DLC flaps, each driven by an individual electrohydraulic actuation system. In the present case, differences up to 6 deg are allowed without automatically switching over from the fly-by-wire mode to the basic mode. Such unequal deflections are also observed in Fig. 6 during typical dynamic flight maneuvers with 3211 DLC inputs, which are used for estimation of the DLC-flap effectiveness. The 3211 input sequence consists of steps of 3, 2, 1, and 1 units of time duration in alternate directions, respectively. This multistep

input signal provides the system with excitation over a fairly broad, flat-frequency range, and is found to be superior for aircraft parameter estimation applications.[17,18]

As a result of unsymmetries in the possible maximum deflection, larger commanded inputs may result in different left and right DLC-flap deflections, leading to unequal lift and drag forces on the two sides of the wing. These unequal forces, assumed to be acting through the center of each of the surfaces away from the aircraft centerline, result in rolling and yawing moments.

Figure 6 shows two flight maneuvers, the first being an aileron-input maneuver in which a rapidly changing 3211 input is applied to ailerons at zero DLC-flap deflection, and the second being a DLC-input maneuver in which a 3211 input is applied to the DLC-flaps without commanding any aileron deflection. This figure shows that during the first maneuver, except for a small bias of about 0.5 deg which remains constant throughout the maneuver, the variations in the left and right aileron deflections are equal, as is generally expected. On the other hand, during the second maneuver, it is clearly observed that the variations in the aerodynamic loads due to DLC-flap deflections result in unequal deflections of the left and right aileron surfaces, leading to control surface interference effects.

Based on the foregoing brief discussion on modeling of coupling effects due to unsymmetries in the DLC-flaps deflection and also the control surface interference effects, the variations in rolling and yawing moment coefficients due to the DLC flaps are modeled as

$$\Delta C_{l\mathrm{DLC}} = (\Delta C^{L}_{\mathrm{LDLC}} - \Delta C^{R}_{\mathrm{LDLC}}) \frac{l_{\mathrm{DLC}}}{s} + C_{l\xi\eta_{\mathrm{DLC}}} \xi\eta_{\mathrm{DLC}} \quad (7a)$$

$$\Delta C_{n\mathrm{DLC}} = (\Delta C^{R}_{\mathrm{DDLC}} - \Delta C^{L}_{\mathrm{DDLC}}) \frac{l_{\mathrm{DLC}}}{s} + C_{n\xi\eta_{\mathrm{DLC}}} \xi\eta_{\mathrm{DLC}} \quad (7b)$$

where l_{DLC} is the lever arm, i.e., the distance along the y axis from the aircraft centerline to aerodynamic center of the DLC flaps, s equal to half the wing span is the reference length for lateral-directional variables, and ξ is the aileron deflection. The first term on the right side of Eqs. (7a) and (7b), computed from the lift and drag differentials, account for the rolling and yawing moment contributions without defining additional derivatives. In addition, it also provides an option to estimate the lever arm l_{DLC}. The derivatives $C_{l\xi\eta_{\mathrm{DLC}}}$ and $C_{n\xi\eta_{\mathrm{DLC}}}$ model the control surface interference effects.

Estimation of the DLC derivatives is carried out by combining several maneuvers with 3211 DLC inputs at different reference flights. For illustration purposes, however, only two typical maneuvers are selected. The control inputs applied during the two maneuvers are shown in Fig. 7. The elevator and rudder deflections are denoted by η and ζ, respectively. In the first maneuver, two 3211 input sequences with different amplitudes are applied, the first one resulting in an almost

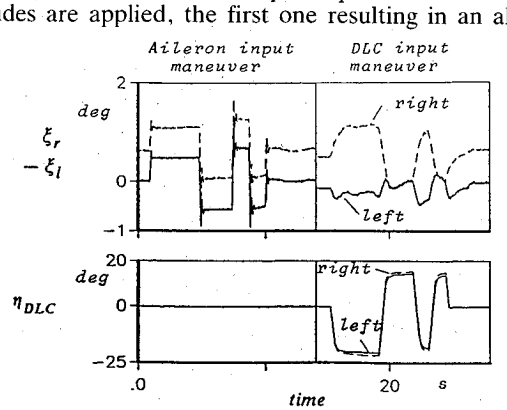

Fig. 6 Flight-measured aileron and DLC-flap deflections.

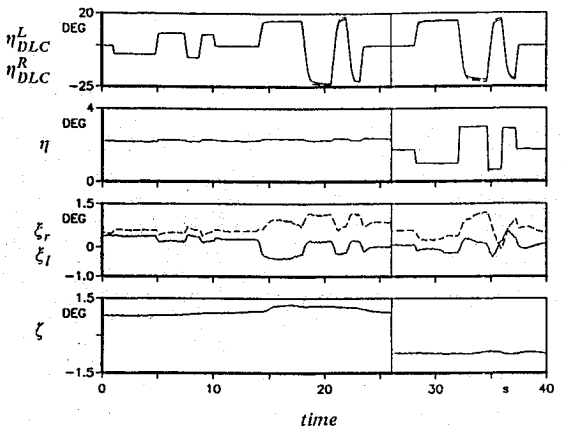

Fig. 7 Identification of DLC-flap effectiveness—flight measured control inputs.

symmetrical deflection of about ±8 deg for both left and right DLC flaps, and the second resulting in a maximum deflection which is limited. During the second maneuver again a number of 3211 sequences of different input amplitudes are applied simultaneously to elevator and DLC flaps.[12] However, only a single 3211 sequence is shown in Fig. 7, clearly indicating the unequal deflections of the right and left DLC flaps. During these two maneuvers, no specific control inputs are applied to the aileron and rudder.

The effectiveness of the DLC flaps is identified based on two different model postulates. The results are presented for the two cases in Figs. 8a and 8b supplemented by Fig. 9. In the first case, the aerodynamic effectiveness is estimated based on Eqs. (4a–c) without the term $\Delta C^{\epsilon}_{m\mathrm{DLC}}$ and Eqs. (5) only, i.e., neglecting the downwash lag effect as modeled in Eq. (6) and also neglecting the rolling and yawing moments due to the unsymmetrical and interference effects of the DLC flaps as modeled in Eqs. 7. In the second case, these effects as postulated in Eqs. (4–7) are accounted for.

A study of the longitudinal motion variables in Figs. 8 and 9 leads to some interesting conclusions. The basic aerodynamic model for effectiveness of the DLC flaps, postulated in Eqs. (5), is identified in these cases. The response match for the horizontal and vertical accelerations, a_x and a_z, as well as for the angle of attack α is found to be fairly good. The postulated cubic model for the lift and quadratic model for the drag is therefore considered adequate. On the other hand, the match for the pitch rate q in Fig. 8a shows some very discernible discrepancies. This figure and the time-expanded plot in Fig. 9a for a single 3211 sequence show that the match between the flight measured and estimated responses for steady-state levels is acceptable, but that for dynamic changes from one steady-state level to another show larger deviations.

An iterative model identification procedure showed that a lag in the downwash due to the DLC-flap deflection significantly affects the aircraft pitching moment.[12] By analogy to the translational acceleration derivatives derived from approximations of unsteady aerodynamic effects[18,19] (in particular, the derivative $C_{m\dot{\alpha}}$ modeling the downwash lag due to variations in the angle of attack), in the present case the downwash lag due to DLC-flap deflection can be approximated through a first-order linear pitching moment derivative with respect to rate of change of DLC-flap deflection $\dot{\eta}_{\mathrm{DLC}}$. However, estimation of such derivatives applying a parameter estimation method would either require a measurement of $\dot{\eta}_{\mathrm{DLC}}$ or computation of the same from measured deflection η_{DLC} by numerical differentiation in a data preprocessing step prior to parameter estimation.

Alternatively, the downwash lag effect can be accounted for by using a time-delayed signal in parameter estimation. Although a first-order filter is commonly used to model time delays,[20] in the present case it will only be an approximation

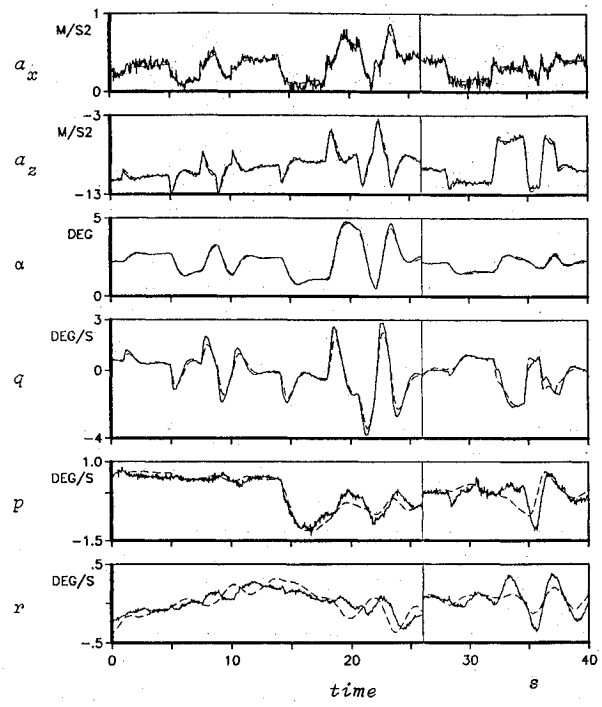

a) Neglecting unsymmetrical, interference, and downwash effects

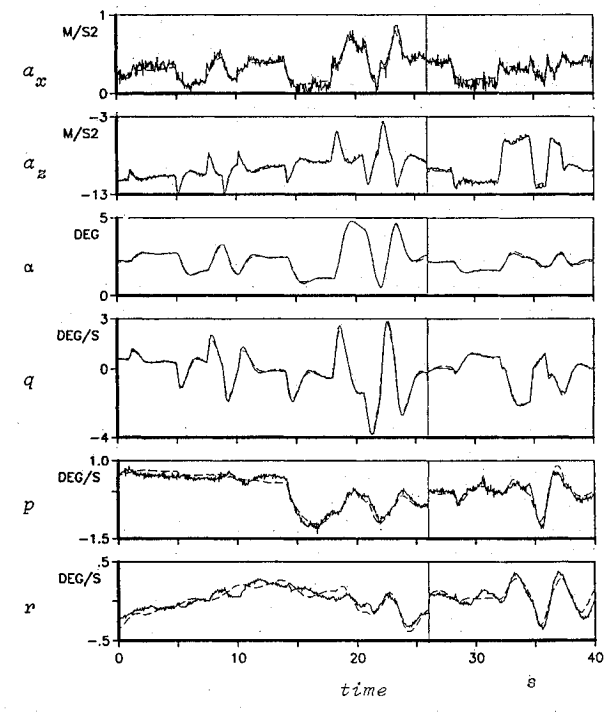

b) Accounting for unsymmetrical, interference, and downwash effects

Fig. 8 Identification of DLC-flap effectiveness: (——flight measured; ------ estimated).

to the actual phenomenon of transit-time effect. The transit-time effects can be more realistically and explicitly accounted for through a delay matrix. Therefore, as postulated in Eq. (6), the second alternative is adopted in the present investigations. This approach, however, requires an estimation program capable of handling nonlinear system models as well as a provision to generate a time delay in a specified variable—in the present case η_{DLC}. Both of these options are available in the estimation program used in the current investigations.[21,22] The improvements observed in the match for the pitch rate in Figs. 8b and 9b are, without any further explanation, self-illustrative of the downwash lag effect. The cubic

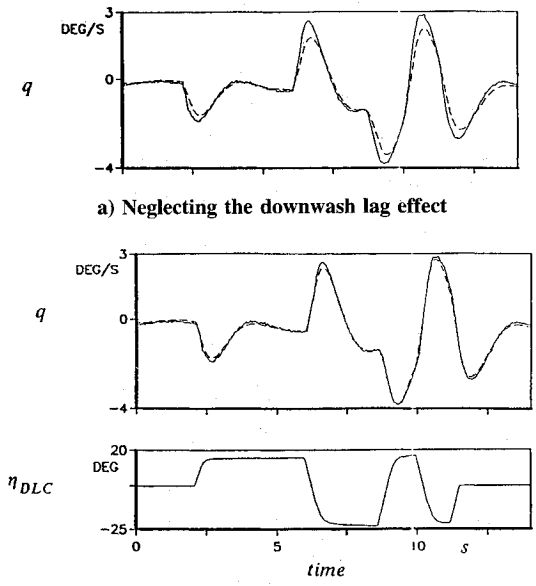

Fig. 9 Measured (——) and estimated (------) pitch rate in response to DLC-flap input.

model for the pitching moment due to DLC flaps in Eqs. (5) thus needs to be augmented with Eq. (6) for the downwash lag effect.

To avoid the problems of linear dependence among the parameters of Eqs. (5) being estimated, large DLC-flap deflections resulting in nonlinear characteristics were necessary. As already mentioned, both small input amplitudes as well as those resulting in maximum deflections (Fig. 7) were analyzed. The maximum likelihood estimation procedure provided the Cramer-Rao bounds of less than 2% for the estimated DLC derivatives.[12] In general, it is known that the Cramer-Rao bounds provide usually optimistic estimates of the accuracy of the estimated parameters. To obtain a realistic value for the error bounds, a fudge-factor of 5–10 is recommended.[16] Under this practical consideration the values for the accuracy of the estimated-parameters are also found to be reasonable.

An attempt to simultaneously estimate the longitudinal derivatives and DLC derivatives neglecting the downwash due to DLC-flap deflection from DLC-input maneuvers, although yielding an acceptable match between the flight measured and estimated pitch rate response, is found to affect the estimates of certain derivatives. In particular, the estimate of pitch-damping derivative C_{mq} is much higher than would otherwise be obtained from the pure longitudinal maneuvers with only elevator and stabilizer inputs. Only by including the downwash lag due to DLC-flap deflection, is this derivative, as well as others are, accurately estimated. Similar influence of unsteady aerodynamics on the flight-extracted derivatives has also been observed in the past.[23,24]

Furthermore, some unmodeled effects in the rolling and yawing motion are clearly observed in Fig. 8a from the match for p, the roll rate and r, the yaw rate, respectively. A comparison with Fig. 8b clearly shows that the rolling moment due to unequal deflections of the DLC flaps as modeled in Eq. (7a) leads to a much-improved match for the roll rate. The change in rolling moment coefficient computed in Eq. (7a) from the lift differential is found to contribute mainly to the improvements observed. The improvements in the roll response match resulting from the derivative $C_{l\xi\eta_{DLC}}$ were in qualitative nature minor, nevertheless this derivative is consistently estimated with a low standard deviation of less than 2%. It can be interpreted as an influence of the DLC flaps on the aileron effectiveness. It is also interesting to note that the average estimated value of 3.94 m for the lever arm l_{DLC}

agrees very well with 4.05 m, the geometrical midpoint of the DLC flaps.

The improvement in the match for the yaw rate r, particularly for the second maneuver in Fig. 8b, is obtained through the derivative $C_{n\xi\eta_{DLC}}$. It results mainly from the control surface interference effects. It is consistently estimated with a low standard deviation of less than 2% for all of the DLC maneuvers analyzed. On the other hand, it is worth noting that it was not possible to estimate the conventional derivative $C_{n\xi}$ (i.e., the change in yawing moment coefficient due to variation in aileron deflection) from the pure lateral-directional flight maneuvers and was, therefore, set to zero. The yawing moment contribution due to the drag differential resulting from DLC-flap deflections, as computed in Eq. (7b), is found to result in only minor improvements in the match for the yaw rate. Nevertheless, Eq. (7b) includes this contribution for the sake of completeness.

Other types of interference effects of active control surfaces have also been observed in the past. For example, a nonlinear interference effect between DLC flaps and spoilers,[6] active side-force control resulting in adverse lift and drag modulation due to flow separation,[25] and side-force generator affecting the stability and control parameters.[26]

Model Validation

Validation of the identified model is an integral part of the system identification and plays an important role in establishing the adequacy and accuracy of the model. A graphical comparison of the measured and estimated response provides a qualitative measure, and the determinant of the covariance matrix of the residuals the quantitative relative measure of the goodness of fit. The standard deivations (Cramer-Rao bounds) and the correlation coefficients help to determine the accuracies of the various parameter estimates. A comparison of the estimates with the wind tunnel or analytical predictions and a check on the plausibility of the estimates from the physical understanding of the system under investigation helps to further gain confidence in the identified model. These criteria, although being useful in many cases, are not enough to guarantee the validity of the model over the entire range of operation.

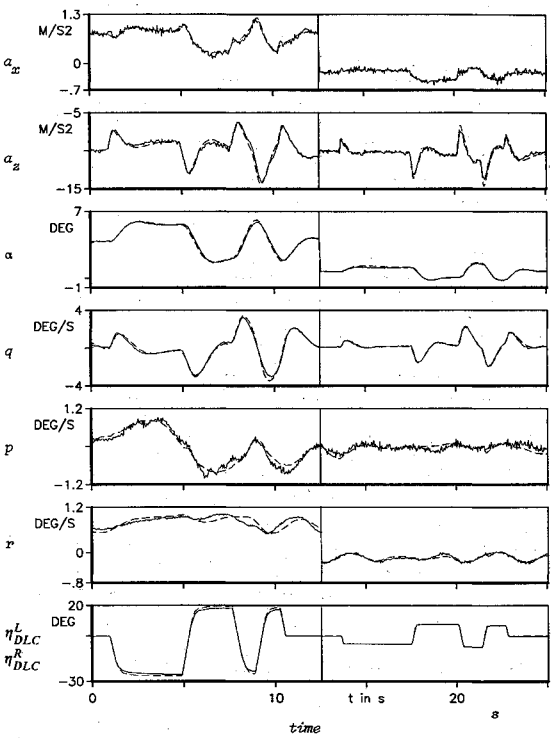

Fig. 10 Prediction capability of the identified model: (——flight measured; ------predicted).

A common approach to further validate the model is to verify the predictive capability of the identified model. For this purpose, the identified model is used to predict the system responses at flight conditions or over the time records not used in parameter estimation. For example, in the present case Fig. 10 shows the predictive capability of the identified model. Both of the time segments were not used in the parameter estimation, in addition, the second one is at different flight conditions than those analyzed for parameter estimation. The aerodynamic derivatives are kept fixed, estimating only the initial conditions to account for the change in flight condition. For both small and large deflections, the overall match between the flight measured and predicted variables is found to be good. Based on the good prediction capability of the model and the fact that the estimates are uncorrelated with very low standard deviations, it can be concluded that the identified model adequately characterizes the DLC flaps.

Comparison of Aerodynamic Characteristics

The aerodynamic characteristics estimated from flight data by system identification methods are compared in Fig. 11 with those predicted by wind tunnel and analytical methods for two landing flap positions, η_k = 1 and 14 deg. In general, it has been observed that the estimated lift coefficient C_{LDLC} is smaller than the predicted (Fig. 11a). The difference is pronounced for larger positive, i.e., downward, deflections of the DLC flaps. Even for the relatively smaller positive DLC-flap deflections of 10–20 deg, the influence of flow separation is evident for landing-flap deflection of η_k = 14 deg. It is therefore identified that the DLC flaps are somewhat less effective in generating the direct-lift than designed for and predicted from the wind-tunnel measurements.

The predicted pitching moment characteristics due to the DLC flaps agree reasonably well with the estimated characteristics, see Fig. 11b. Some deviations are observed for larger

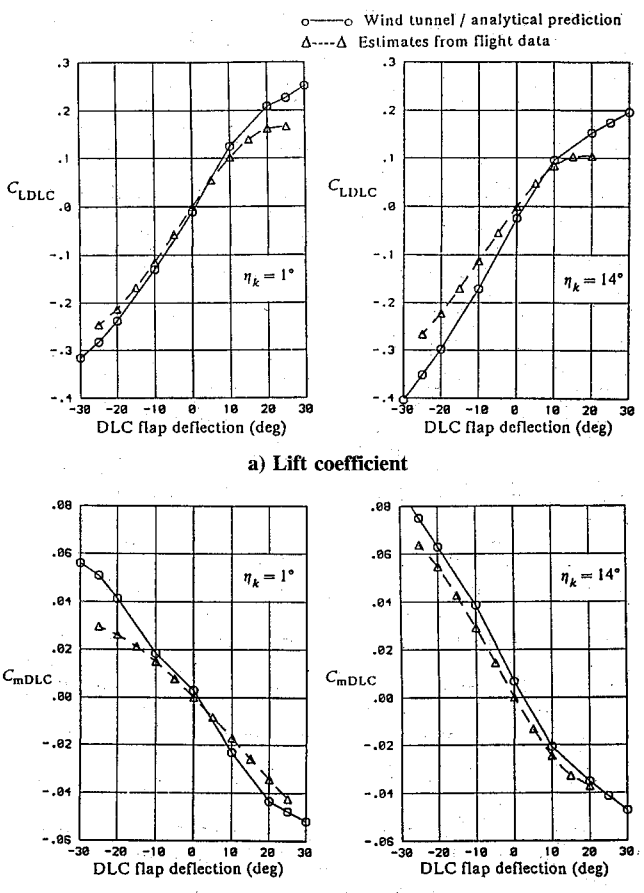

Fig. 11 Effectiveness of DLC flaps (static characteristics).

flap deflection at $\eta_k = 1$ deg. The agreement is particularly good for the landing-flap position of $\eta_k = 14$ deg, except for a shift, which is attributed to the differences in the aerodynamic bias term C_{m0}, which is of little interest.[12] Although the differences in the estimated and predicted pitching moment coefficient are not large, it is to be remembered here that Fig. 11b shows only static characteristics. It accounts for the downwash effect, but only when a steady state is reached. In the previous section, it has already been demonstrated that the transient effects of the downwash lag has a significant influence on the pitching moment response for both small and large deflections of the DLC flaps, see Fig. 8 and 9. Such dynamic influences must be considered in addition to the static characteristics shown in Fig. 11b.

Concluding Remarks

The system identification methodology has been successfully applied to derive from flight test data the models for actuation systems and for aerodynamic characteristics of the specially designed direct-lift-control flaps. By way of an example, it is shown that the possible maximum deflection of these flaps is severely limited under aerodynamic loads. Furthermore, the different actuation systems for the six DLC flaps can possibly lead to unequal deflections of the DLC flaps, which are otherwise configured for symmetrical deflections. A control surface interference effect between the DLC flaps and ailerons has also been observed. The flight-estimated aerodynamic characteristics are compared with those predicted by wind tunnel and analytical methods. The aerodynamic estimation from flight data clearly showed that the DLC flaps are somewhat less effective than designed for. Moreover, it has been shown that the downwash lag effect due to deflection of the DLC flaps plays a dominant role not only in the steady state but also in the transient response, significantly affecting the dynamic motion in the pitching mode. The improvements in the parameter estimation results obtained by accounting for the unsteady, unsymmetrical, and interference effects of the DLC flaps are demonstrated.

Appendix: Parameter Estimation Algorithm

The research and development work on system identification methodology at the DLR has resulted in several parameter estimation programs capable of analyzing dynamic systems with different degrees of complexities.[11,13,21] For the investigations reported in this article, the NLHPXL computer program is applied to estimate the aerodynamic parameters.[22] This more routinely used estimation program is based on the maximum likelihood principle and is applicable to general nonlinear systems whose output measurements are corrupted by noise.

The estimation of parameter values from measured aircraft responses to given control inputs requires a mathematical model of the aircraft to be postulated. In a general form, the equations of aircraft motion can be written as

$$\dot{\boldsymbol{x}}(t) = \boldsymbol{f}[\boldsymbol{x}(t), \boldsymbol{X}(t, \tau), \boldsymbol{u}(t) - \Delta\boldsymbol{u}(b_{u,l}), \boldsymbol{U}(t, \tau), \beta], \quad \boldsymbol{x}(t_{0,l}) = \boldsymbol{x}_0(b_{x,l}) \tag{A1a}$$

$$\boldsymbol{y}(t) = \boldsymbol{g}[\boldsymbol{x}(t), \boldsymbol{X}(t, \tau), \boldsymbol{u}(t) - \Delta\boldsymbol{u}(b_{u,l}), \boldsymbol{U}(t, \tau), \beta] + \Delta\boldsymbol{z}(b_{y,l}) \quad l = 1, \ldots, nz \tag{A1b}$$

$$\boldsymbol{z}(t_k) = \boldsymbol{y}(t_k) + G\boldsymbol{v}(t_k) \quad k = 1, \ldots, N \tag{A1c}$$

where $\boldsymbol{x}$ is the $(n \times 1)$ state vector, $\boldsymbol{u}$ the $(p \times 1)$ control input vector, $\boldsymbol{y}$ the $(m \times 1)$ observation (model output) vector, k is the discrete time index, and l is the index for time segment being analyzed. The n- and m-dimensional system functions f and g are general nonlinear real valued vector functions. The measurement vector $\boldsymbol{z}$ is sampled at N discrete time points. The measurement noise vector $\boldsymbol{v}$ is assumed to be characterized by a sequence of independent Gaussian random variables with zero mean and identity covariance. The matrices $X(t, \tau)$ and $U(t, \tau)$ denote the matrices of the time-delayed state and input variables with

$$[X(t, \tau)]_{ij} = \boldsymbol{x}_i(t - \tau_j) \tag{A2a}$$

$$[U(t, \tau)]_{ij} = \boldsymbol{u}_i(t - \tau_j) - \Delta\boldsymbol{u}(b_{u,l}) \tag{A2b}$$

Note that the postulated model includes nz time records to be analyzed simultaneously. Furthermore, β represents the unknown system coefficients, τ denotes the unknown time delays, $\boldsymbol{x}_0$ denotes the unknown initial conditions, and $\Delta\boldsymbol{z}$ and $\Delta\boldsymbol{u}$ denote the possible zero shifts in the measurements of the output and control variables. In general, not all of the components of $\boldsymbol{x}_0$, $\Delta\boldsymbol{z}$, and $\Delta\boldsymbol{u}$ can be estimated since they may be linearly dependent or highly correlated. The corresponding components which can be estimated are denoted by $b_{x,l}$, $b_{y,l}$, and $b_{u,l}$ for the lth time segment, respectively. The complete parameter vector $\boldsymbol{\Theta}$ to be estimated in such a case is given by

$$\{\boldsymbol{\Theta}\}^T = \{\beta^T; \tau^T, b_{x,l}^T, \ldots, b_{x,nz}^T; b_{y,1}^T, \ldots, b_{y,nz}^T; b_{u,1}^T, \ldots, b_{u,nz}^T\} \tag{A3}$$

The maximum likelihood estimates of $\boldsymbol{\Theta}$ are obtained by minimizing the negative logarithm of the likelihood function[10,11]

$$J(\boldsymbol{\Theta}) = \frac{1}{2}\sum_{k=1}^{N}[\boldsymbol{z}(t_k) - \boldsymbol{y}(t_k)]^T R^{-1}[\boldsymbol{z}(t_k) - \boldsymbol{y}(t_k)] + \frac{N}{2}\ln|R| \tag{A4}$$

where R is the covariance matrix of the residuals. Minimization is carried out subject to the postulated system model, Eqs. (A1–A2). Starting from the suitably specified initial values of $\boldsymbol{\Theta}$, the estimates are iteratively updated using the Gauss-Newton method. The sensitivity coefficients required in the optimization procedure are obtained by finite-difference approximation.[13]

Acknowledgments

This work was carried out in cooperation with special research project SFB-212, "Safety in Aviation," Technical University of Braunschweig. It was partly sponsored by the Deutsche Forschungsgemeinschaft, DFG. Their support is gratefully acknowledged.

References

[1]Hanke, D., "Der Fliegende Simulator und Technologieträger ATTAS der DFVLR," Luft- und Raumfahrt, Vol. 7, Jan. 1986, pp. 4–8.

[2]Hanke, D., Wilhelm, K., and Meyer, H.-L., "Development and Applications of In-Flight Simulator Aircraft for Flying Qualities Research at DFVLR," *Proceedings of the NAECON '86 Symposium on "Developing Technologies for Revolutionary Applications."* Paper 117, Dayton, OH, May 19–23, 1986.

[3]König, R., and Hahn, K.-U., "Load Alleviation and Ride Smoothing Investigations Using ATTAS," International Council of the Aeronautical Sciences 90-5.7.4, Stockholm, Sweden, Sept. 1990.

[4]Wilhelm, K., and Hahn, K.-U., "ATTAS—Recent Flying Qualities Experiments," International Symposium on "In-Flight Simulation for the 90's," German Aerospace Research Establishment, Braunschweig, Germany, July 1–3, 1991.

[5]Smith, R. E., "Flying Qualities Development for the X-29A Demonstrator," International Symposium on "In-Flight Simulation for the 90's," German Aerospace Research Establishment, Braunschweig, Germany, July 1–3, 1991.

[6]Hamel, P. G., "Determination of Aircraft Dynamic Stability and Control Parameters from Flight Testing," AGARD LS-114, 1981, pp. 10-1–10-42.

[7]Iliff, K. W., "Parameter Estimation for Flight Vehicles," *Journal of Guidance, Control, and Dynamics*, Vol. 12, Sept.–Oct. 1989, pp. 609–622.

[8]Klein, V., "Estimation of Aircraft Aerodynamic Parameters from Flight Data," *Progress in Aerospace Sciences*, Vol. 26, Jan. 1989, pp. 1–77.

[9]Chetty, S., and Henschel, F., "Model Following Control System Design—Preliminary ATTAS Inflight Simulation Test Results," DLR-IB 111-89/39, Braunschweig, Germany, Dec. 1989.

[10]Maine, R. E., and Iliff, K. W., "Identification of Dynamic Systems," AGARD AG-300, Vol. 2, Jan. 1985.

[11]Jategaonkar, R. V., and Plaetschke, E., "Algorithms for Aircraft Parameter Estimation Accounting for Process and Measurement Noise," *Journal of Aircraft*, Vol. 26, No. 4, 1989, pp. 360–372.

[12]Jategaonkar, R. V., "Determination of Aerodynamic Characteristics from ATTAS Flight Data Gathering for Ground-Based Simulator," DLR-FB 91-15, Braunschweig, Germany, May 1991.

[13]Jategaonkar, R. V., and Plaetschke, E., "Maximum Likelihood Parameter Estimation from Flight Data for General Nonlinear Systems," DFVLR-FB 83-14, April 1983.

[14]Rohlf, D., and Mönnich, W., "Zur Identifizierung des DLC-Klappensystems des Forschungsfluzeugs ATTAS," Symposium "Systemidentifizierung in der Fahrzeugdynamik," DFVLR-Mitt. 87-22, Paper 3.2, Dec. 1987.

[15]Lange, H.-H., Rohlf, D., Zach, A., and Meyer, H.-L., "ATTAS Flight Testing Experience," AGARD CP-452, July 1989, pp. 2-1–2-14.

[16]Maine, R. E., and Iliff, K. W., "Identification of Dynamic Systems—Applications to Aircraft. Part 1: The Output Error Approach," AGARD-AG-300, Vol. 3, Pt. 1, Dec. 1986.

[17]Plaetschke, E., Mulder, J. A., and Breeman, J. H., "Results of Beaver Aircraft Parameter Estimation," DFVLR-FB 83-10, March 1983.

[18]Maine, R. E., and Iliff, K. W., "Maximum Likelihood Estimation of Translational Acceleration Derivatives from Flight Data," *Journal of Aircraft*, Vol. 16, No. 10, 1979, pp. 674–679.

[19]Jategaonkar, R. V., and Gopalratnam, G., "Two Complementary Approaches to Estimate Downwash Lag Effects from Flight Data," *Journal of Aircraft*, Vol. 28, No. 8, 1991, pp. 540–542.

[20]Zerweckh, S. H., and von Flotow, A. H., "Flight Testing a Highly Flexible Aircraft: Case Study on the MIT Light Eagle," AIAA Paper 88-4375-CP, AIAA Atmospheric Flight Mechanics Conf., Minneapolis, MN, Aug. 15–17, 1988.

[21]Plaetschke, E., "Ein FORTRAN-Programm zur Maximum-Likelihood-Parameterschätzung in nichtlinearen retardierten Systemen der Flugmechanik—Benutzeranleitung," DFVLR-Mitt. 86-08, March 1986.

[22]Weiß, S., "NLHP1L: Ein Programm zur Maximum-Likelihood-Parameterschätzung für nichtlineare Systeme—Benutzeranleitung," DFVLR-IB 111-87/29, July 1987.

[23]Wells, W. R., and Queijo, M. J., "Simplified Unsteady Aerodynamic Concepts with Application to Parameter Estimation," *Journal of Aircraft*, Vol. 16, No. 2, 1979, pp. 90–94.

[24]Queijo, M. J., Wells, W. R., and Keskar, D. A., "The Influence of Unsteady Aerodynamics on Extracted Aircraft Parameters," AIAA Paper 78-1343, 1978.

[25]Anon., "Total In-Flight Simulator (TIFS)—Preliminary Design Report," Air Force Flight Dynamics Lab., TR 71-119, Aug. 1971, pp. 25–26.

[26]Smith, H. J., "Flight Determined Stability and Control Derivatives for an Executive Jet Transport," NASA TMX-56034, July 1975.